



**HAL**  
open science

# Numerical Analysis of Nonlocal Anisotropic Continuum Damage

Sabine Ricci, Michael Brünig

► **To cite this version:**

Sabine Ricci, Michael Brünig. Numerical Analysis of Nonlocal Anisotropic Continuum Damage. International Journal of Damage Mechanics, 2007, 16 (3), pp.283-299. 10.1177/1056789506064947 . hal-00571159

**HAL Id: hal-00571159**

**<https://hal.science/hal-00571159>**

Submitted on 1 Mar 2011

**HAL** is a multi-disciplinary open access archive for the deposit and dissemination of scientific research documents, whether they are published or not. The documents may come from teaching and research institutions in France or abroad, or from public or private research centers.

L'archive ouverte pluridisciplinaire **HAL**, est destinée au dépôt et à la diffusion de documents scientifiques de niveau recherche, publiés ou non, émanant des établissements d'enseignement et de recherche français ou étrangers, des laboratoires publics ou privés.

# Numerical Analysis of Nonlocal Anisotropic Continuum Damage

SABINE RICCI\* AND MICHAEL BRÜNIG

*Lehrstuhl für Baumechanik - Statik, Universität Dortmund  
August-Schmidt-Str. 6, D-44221 Dortmund, Germany*

**ABSTRACT:** This article deals with the numerical analysis of anisotropic continuum damage in ductile metals based on thermodynamic laws and nonlocal theories. The proposed model is based on a generalized macroscopic theory within the framework of nonlinear continuum damage mechanics taking into account the kinematic description of the damage. A generalized yield condition is employed to describe the plastic flow characteristics of the matrix material, whereas the damage criterion provides a realistic representation of material degradation. The nonlocal theory of inelastic continua is established, which incorporates the macroscopic interstate variables and their higher-order gradients which properly describe the change in the internal structure and investigate the size effect of statistical inhomogeneity of the heterogeneous material. The idea of bridging length scales is made by using the higher-order gradients only in the evolution equations of the equivalent inelastic strain measures. This leads to a system of elliptic partial differential equations which is solved using the finite difference method. The applicability of the proposed continuum damage theory is demonstrated by finite element analyses of the inelastic deformation process of tension specimens.

**KEY WORDS:** elastic-plastic material, anisotropic damage, nonlocal material model, finite strains, finite difference method, finite element analyses.

## INTRODUCTION

**T**HE ACCURATE AND realistic description of inelastic behavior of ductile materials as well as the development of associated efficient and stable numerical solution techniques are essential for the solution of numerous boundary-value problems occurring in engineering. The nonlinear material behavior is caused by two distinct material processes: (i) dislocations along

---

\*Author to whom correspondence should be addressed. E-mail: sabine.ricci@uni-dortmund.de

distinct crystal slip planes and (ii) the evolution and growth of microcavities and microcracks. These two completely different degradation phenomena are adequately described by the continuum theories of plasticity and damage mechanics.

Classical local continuum theories are based on the assumption that, at a given point, the physical state of a body is completely determined by the state of the material lying within an arbitrarily small neighborhood of that point. Such local material models have been successfully used in describing the macroscopic stress and strain fields in a large number of engineering problems. Nonlocal effects, on the other hand, are important when deformation mechanisms governed by microscopic phenomena as well as scale effects have to be considered in order to explain and predict certain experimentally observed critical phenomena. For example, nonlocal theories represent a constitutive framework on the continuum level that is used to bridge the gap between the micromechanical level and the classical continuum level through the incorporation of intrinsic material length parameters into the constitutive model. This is made by using spatial higher-order gradients in the evolution equations of the respective internal state variables describing plastic and damage growth.

The present article discusses a finite strain framework for ductile anisotropic continuum damage and presents a numerical approach where the gradient-enhanced constitutive model leads to a system of elliptic partial differential equations for the internal variable which is solved using the finite difference method; whereas the displacement-based finite element procedure is governed by the standard principle of virtual work. The applicability of the proposed continuum damage theory is demonstrated by finite element analyses of the inelastic deformation process of tension specimens.

## FUNDAMENTAL GOVERNING EQUATIONS

In the past decades, the constitutive modeling of ductile damaged solids in the finite deformation range has received considerable attention. For example, scalar-valued damage variables have been proposed by Kachanov (1958), Lemaitre (1985a,b), and Tvergaard (1990) among many others. To be able to take into account the damage-induced material anisotropy, damage tensors have been introduced e.g., by Murakami and Ohno (1981), Krajcinovic (1983), Chaboche (1988a,b), Murakami (1988), Ju (1990), Voyiadjis and Kattan (1992), Abu Al-Rub and Voyiadjis (2003), and Hammi et al. (2003, 2004).

The framework presented by Brünig (2003a,b) is used to describe the inelastic deformations including anisotropic damage due to microdefects.

Briefly, the kinematic description employs the consideration of damaged as well as fictitious undamaged configurations related via metric transformations which allow for the definition of damage strain tensors  $\mathbf{A}^{\text{da}}$ . The modular structure is accomplished by the kinematic decomposition of strain rates,  $\dot{\mathbf{H}}$ , into elastic,  $\dot{\mathbf{H}}^{\text{el}}$ , effective plastic,  $\dot{\mathbf{H}}^{\text{pl}}$ , and damage parts,  $\dot{\mathbf{H}}^{\text{da}}$ .

To be able to address equally the two physically distinct modes of irreversible changes, i.e., plastic flow and damage, respective Helmholtz free energy functions with respect to the fictitious undamaged and to the current damaged configurations are introduced separately. The effective specific free energy  $\bar{\phi}$  of the fictitious undamaged matrix material is assumed to be additively decomposed into an effective elastic and an effective plastic part

$$\bar{\phi} = \bar{\phi}^{\text{el}}(\bar{\mathbf{A}}^{\text{el}}) + \bar{\phi}^{\text{pl}}(\tilde{\gamma}) \tag{1}$$

where  $\bar{\mathbf{A}}^{\text{el}}$  is the logarithmic effective elastic strain tensor. In Equation (1),  $\tilde{\gamma}$  denotes the internal plastic variable

$$\tilde{\gamma} = (1 - m_{\text{pl}})\gamma + m_{\text{pl}}\hat{\gamma} \tag{2}$$

where  $\gamma$  is a local internal mechanical state variable characterizing plastic deformation behavior and  $\hat{\gamma}$  represents its nonlocal counterpart. The parameter  $m_{\text{pl}}$  in Equation (2) denotes the relative weight of the local plastic effects compared to the nonlocal ones. If  $m_{\text{pl}}=0$ , Equation (2) reduces to the standard local plastic constitutive relationship discussed by Brünig (1999) whereas for  $m_{\text{pl}}=1$ , one obtains a purely nonlocal formulation. The nonlocal internal variable plays the role of an explicit link between the plastic hardening at the microscale and the behavior of the homogeneous equivalent material at the macroscale. The use of the nonlocal theory is made to achieve this long-range microstructural interaction. Nonlocal effects are described via additional length quantities which play the role of material parameters (Abu Al-Rub and Voyiadjis, 2004) and are used to obtain weighted averages of the corresponding local variables over a material volume of the body. In particular, the nonlocal equivalent plastic strain  $\hat{\gamma}$  is taken to be a volume average of the corresponding local variable over a fixed and isotropic representative volume element surrounding the considered material point. The volume average of  $\gamma$  at a location  $\mathbf{x}$  is defined as

$$\hat{\gamma}(x) = \frac{1}{V_{\text{pl}}(\mathbf{x})} \int \alpha_{\text{pl}}(\mathbf{x} - \mathbf{s}) \gamma(\mathbf{s}) \, d\mathbf{s}, \tag{3}$$

where

$$V_{\text{pl}}(\mathbf{x}) = \int \alpha_{\text{pl}}(\mathbf{x} - \mathbf{s}) \, d\mathbf{s} \quad (4)$$

denotes a representative volume,  $\mathbf{x}$  and  $\mathbf{s}$  are coordinate vectors, and the plastic averaging function  $\alpha_{\text{pl}}$ , which has a maximum at  $\mathbf{x} = \mathbf{s}$ , decays smoothly with distance and is symmetric about this maximum, and implicitly contains an intrinsic characteristic plastic length  $l_{\text{pl}}$ . Physical and micromechanical arguments suggest that the representative volume should be sufficiently small. In numerical applications, good convergence is obtained when  $\alpha_{\text{pl}}$  is the Gaussian bell curve (Strömberg and Ristinmaa, 1996).

$$\alpha_{\text{pl}}(\mathbf{x}) = \exp \left[ - \left( \frac{k \|\mathbf{x}\|}{l_{\text{pl}}} \right)^2 \right]. \quad (5)$$

In Equation (5), the internal plastic length parameter  $l_{\text{pl}}$  determines the range of the function  $\alpha_{\text{pl}}$ , and for the one-, two-, and three-dimensional cases,  $\|\mathbf{x}\|$  and  $k$  are given by

$$\begin{aligned} 1D: \quad & \|\mathbf{x}\| = x; \quad k = \sqrt{\pi} \\ 2D: \quad & \|\mathbf{x}\| = \sqrt{x^2 + y^2}, \quad k = 2 \\ 3D: \quad & \|\mathbf{x}\| = \sqrt{x^2 + y^2 + z^2}, \quad k = (6\sqrt{\pi})^{1/3}, \end{aligned} \quad (6)$$

where  $x$ ,  $y$ , and  $z$  denote Cartesian coordinates (Brünig et al. (2001)). Physically, the characteristic plastic length  $l_{\text{pl}}$  represents a material property which is of the order of magnitude of the maximum size of the plastic material inhomogeneities – in the case of crystalline solids, this may be the lattice spacing; whereas in the case of granular materials it may be the grain size. Also, when  $l_{\text{pl}}$  is set equal to zero, the classical local  $I_1$ - $J_2$ - metal plasticity theory presented by Brünig (1999, 2003a) is recovered.

Furthermore, the spatial average  $\hat{\gamma}$  is expanded into a Taylor series about the point  $\mathbf{x}$  and only first- and second-order terms are retained. Carrying out the integration in Equation (3) and using the symmetry requirements for  $\alpha_{\text{pl}}$  (Equation (5)), one arrives at

$$\hat{\gamma} = \gamma + d_{\text{pl}} \frac{\partial^2 \gamma}{\partial \mathbf{x} \cdot \partial \mathbf{x}} + \dots = \gamma + d_{\text{pl}} \nabla^2 \gamma + \dots, \quad (7)$$

where  $d_{\text{pl}}$  is related to  $k$  (Equation (6)), and for the one-, two-, and three-dimensional cases one obtains

$$\begin{aligned} 1D: \quad d_{\text{pl}} &= \frac{l_{\text{pl}}^2}{4\pi} \\ 2D: \quad d_{\text{pl}} &= \frac{l_{\text{pl}}^2}{16} \\ 3D: \quad d_{\text{pl}} &= \frac{l_{\text{pl}}^2}{4\sqrt[3]{36\pi}}. \end{aligned} \quad (8)$$

Taking Equations (2) and (7) into account, the effective plastic part of the Helmholtz free energy function  $\bar{\phi}^{\text{pl}}(\gamma, \nabla^2\gamma)$  (Equation (1)) is an explicit function of both the local plastic internal variable  $\gamma$  and its second-order gradient  $\nabla^2\gamma$ .

Moreover, the thermic state equation leads in the case of isotropic elastic material behavior to the effective stress tensor

$$\bar{\mathbf{T}} = 2G\bar{\mathbf{A}}^{\text{el}} + \left(K - \frac{2}{3}G\right) \text{tr}\bar{\mathbf{A}}^{\text{el}} \mathbf{1} \quad (9)$$

where  $G$  and  $K$  represent the shear and bulk modulus of the matrix material, respectively. In addition, plastic yielding of the hydrostatic stress-dependent matrix material is assumed to be adequately described by the nonlocal yield condition

$$f^{\text{pl}}(\bar{I}_1, \bar{J}_2, c) = \left(1 - \frac{a}{c}\bar{I}_1\right)^{-1} \sqrt{\bar{J}_2} - c(\gamma, \nabla^2\gamma) = 0, \quad (10)$$

where  $\bar{I}_1 = \text{tr}\bar{\mathbf{T}}$  and  $\bar{J}_2 = \frac{1}{2}\text{dev}\bar{\mathbf{T}} \cdot \text{dev}\bar{\mathbf{T}}$  are the invariants of the effective stress tensor  $\bar{\mathbf{T}}$ ,  $c(\gamma, \nabla^2\gamma)$  denotes the gradient-enhanced strength coefficient of the matrix material, and  $a$  represents the hydrostatic stress coefficient.

In addition, in elastic-plastically deformed and damaged metals, irreversible volumetric strains are mainly caused by damage and, in comparison, volumetric plastic strains are negligible. Therefore, the plastic potential function,

$$g^{\text{pl}}(\bar{\mathbf{T}}) = \sqrt{\bar{J}_2} \quad (11)$$

is taken to depend only on the second invariant of the effective stress deviator which leads to the isochoric effective plastic strain rate

$$\dot{\bar{\mathbf{H}}}^{\text{pl}} = \dot{\lambda} \frac{\partial g^{\text{pl}}}{\partial \bar{\mathbf{T}}} = \dot{\lambda} \frac{1}{2\sqrt{\bar{J}_2}} \text{dev}\bar{\mathbf{T}} \quad (12)$$

where  $\dot{\lambda}$  is a nonnegative scalar-valued factor.

In addition, the normalized deviatoric tensor

$$\mathbf{N} = \frac{1}{\sqrt{2\bar{J}_2}} \text{dev}\bar{\mathbf{T}} \quad (13)$$

is introduced which leads to the definition of the equivalent plastic strain rate

$$\dot{\bar{\gamma}} = \mathbf{N} \cdot \dot{\mathbf{H}}^{\text{pl}} = \frac{1}{\sqrt{2}} \dot{\lambda} \quad (14)$$

which will be used to express the plastic strain rate tensor (12) in the form

$$\dot{\mathbf{H}}^{\text{pl}} = \dot{\bar{\gamma}} \mathbf{N}. \quad (15)$$

Moreover, the anisotropically damaged configurations are considered to formulate the constitutive equations which adequately describe the deformation behavior of the damaged aggregate. The complexity of the model is directly determined by the form of the Helmholtz free energy  $\phi$  with respect to the anisotropically damaged configurations and by the number of variables. In particular, dislocations, microvoids, and microcracks are the predominant modes of irreversible microstructural deformations at each stage of the loading process and, therefore, the effects of plastic strain hardening and microdamage mechanisms have to be considered. Pure plastic flow develops by dislocation motion and sliding phenomena along some preferential crystallographic planes whereas damage-related irreversible deformations are due to residual opening of microdefects after unloading. These dissipative processes are distinctly different in their nature and in the manner in which they affect the compliance of the material. In order to take into account plasticity and damage phenomena at a small-scale level in an adequate manner, different internal variables and more than one length parameter should be introduced. Therefore, two sets of internal state variables acting at the microlevel as well as their nonlocal counterparts are chosen characterizing formation of dislocations (plastic internal variables) as well as describing nucleation and propagation of microdefects (damage internal variables).

The Helmholtz free energy of the damaged material sample is assumed to consist of three parts:

$$\phi = \phi^{\text{el}}(A^{\text{el}}, A^{\text{da}}) + \phi^{\text{pl}}(\bar{\gamma}) + \phi^{\text{da}}(\bar{\mu}) \quad (16)$$

with the damage internal variable

$$\tilde{\mu} = (1 - m_{\text{da}})\mu + m_{\text{da}}\hat{\mu}. \quad (17)$$

The elastic free energy  $\phi^{\text{el}}$ , which is an isotropic function of the elastic and damage strain tensors,  $\mathbf{A}^{\text{el}}$  and  $\mathbf{A}^{\text{da}}$ , is used to describe the elastic response of the damaged material at the current state of deformation and material damage (see e.g., Lubarda and Krajcinovic (1995), Hayakawa et al. (1998) and Brünig (2003a)). The plastic and damage Helmholtz free energies depend not only on the macroscopic response associated with the local internal variables  $\gamma$  and  $\mu$ , but also on their nonlocal counterparts  $\hat{\gamma}$  and  $\hat{\mu}$ . In this context,  $\mu$  denotes the local phenomenological internal mechanical state variable describing damage behavior and  $\hat{\mu}$  is its nonlocal counterpart which characterizes the notion of nonuniform distribution of microvoids and microcracks over multiple length scales at which neighbor effects of nonlocal character are significant. The parameter  $m_{\text{da}}$  in Equation (17) denotes the relative weight of the local damage effects compared to the nonlocal ones. If  $m_{\text{da}} = 0$ , Equation (17) reduces to the standard local damage constitutive relationships (Brünig (2003a)) whereas for  $m_{\text{da}} = 1$  one obtains a purely nonlocal formulation.

The nonlocal equivalent damage strain

$$\hat{\mu}(\mathbf{x}) = \frac{1}{V_{\text{da}}(\mathbf{x})} \int \alpha_{\text{da}}(\mathbf{x} - \mathbf{s})\mu(\mathbf{s})\text{d}\mathbf{s}, \quad (18)$$

is – in analogy to  $\hat{\gamma}$  (3) discussed previously – taken to be a volume average of  $\mu$  where

$$V_{\text{da}}(\mathbf{x}) = \int \alpha_{\text{da}}(\mathbf{x} - \mathbf{s})\text{d}\mathbf{s} \quad (19)$$

denotes a representative volume,  $\mathbf{x}$  and  $\mathbf{s}$  are coordinate vectors. The damage averaging function

$$\alpha_{\text{da}}(\mathbf{x}) = \exp\left[-\left(\frac{k\|\mathbf{x}\|}{l_{\text{da}}}\right)^2\right] \quad (20)$$

takes into account an internal damage length scale  $l_{\text{da}}$  representing an effective damage material property which is in the order of magnitude of the maximum size of the material inhomogeneities which may be the microvoid spacing. The parameters  $\|\mathbf{x}\|$  and  $k$  are given in Equation (6). Similar to the

nonlocal plastic variable (Equation (7)), the spatial average  $\hat{\mu}$  is expanded into a Taylor series about the point  $\mathbf{x}$  and only first and second-order terms are retained. Carrying out the integration in Equation (18) and using the symmetry requirements for  $\alpha_{\text{da}}$  (20), one thus arrives at

$$\hat{\mu} = \mu + d_{\text{da}} \frac{\partial^2 \mu}{\partial \mathbf{x} \cdot \partial \mathbf{x}} + \dots = \mu + d_{\text{da}} \nabla^2 \mu + \dots, \quad (21)$$

where  $d_{\text{da}}$  is related to  $l_{\text{da}}$  according to Equation (8). Thus, taking into account Equations (17) and (21), the damage part of the Helmholtz free energy function  $\phi^{\text{da}}(\mu, \nabla^2 \mu)$  (see Equation (16)) is an explicit function of both the local damage internal variable  $\mu$  and its second-order gradient  $\nabla^2 \mu$ .

Furthermore, following Brünig (2003a) the Kirchhoff stress tensor of the damaged material is expressed in the form

$$\begin{aligned} \mathbf{T} = & 2(G + \eta_2 \text{tr} \mathbf{A}^{\text{da}}) \mathbf{A}^{\text{el}} + \left[ \left( K - \frac{2}{3} G + 2\eta_1 \text{tr} \mathbf{A}^{\text{da}} \right) \text{tr} \mathbf{A}^{\text{el}} + \eta_3 (\mathbf{A}^{\text{da}} \cdot \mathbf{A}^{\text{el}}) \right] \mathbf{1} \\ & + \eta_3 \text{tr} \mathbf{A}^{\text{el}} \mathbf{A}^{\text{da}} + \eta_4 (\mathbf{A}^{\text{el}} \mathbf{A}^{\text{da}} + \mathbf{A}^{\text{da}} \mathbf{A}^{\text{el}}) \end{aligned} \quad (22)$$

which is linear in  $\mathbf{A}^{\text{el}}$  and  $\mathbf{A}^{\text{da}}$ , and  $\eta_1, \dots, \eta_4$  are newly introduced material constants taking into account the deterioration of the elastic material properties due to damage.

In analogy to the yield surface and flow rule concepts employed in plasticity theory, evolution of damage is assumed to be adequately described by the nonlocal damage criterion

$$f^{\text{da}}(I_1, J_2, \tilde{\sigma}) = I_1 + \tilde{\beta} \sqrt{J_2} - \tilde{\sigma}(\mu, \nabla^2 \mu) = 0, \quad (23)$$

which is a function of the stress invariants  $I_1 = \text{tr} \mathbf{T} = \text{tr} \tilde{\mathbf{T}}$  and  $J_2 = 1/2 \text{dev} \mathbf{T} \cdot \text{dev} \mathbf{T} = 1/2 \text{dev} \tilde{\mathbf{T}} \cdot \text{dev} \tilde{\mathbf{T}}$  expressed in terms of the stress tensor  $\tilde{\mathbf{T}} = \mathbf{Q}^{\text{el}} \mathbf{T} \mathbf{Q}^{\text{el}-1}$  which is work-conjugate to the damage strain rate tensor  $\dot{\mathbf{H}}^{\text{da}}$  and where  $\mathbf{Q}^{\text{el}}$  represents the elastic metric transformation tensor (see Brünig (2003a) for further details). In addition,  $\tilde{\sigma}(\mu, \nabla^2 \mu)$  denotes the damage threshold which represents the material toughness to microdefect propagation and  $\tilde{\beta}$  characterizes the influence of the deviatoric stress state on the damage condition simulating shear stress instabilities.

To be able to adequately compute damage strain rates, the damage potential function

$$g^{\text{da}}(\tilde{\mathbf{T}}) = \alpha I_1 + \beta \sqrt{J_2} \quad (24)$$

is also formulated in terms of invariants of the stress tensor  $\tilde{\mathbf{T}}$ . In Equation (24)  $\alpha$  and  $\beta$  denote kinematically based damage parameters. This leads to the nonassociated damage rule

$$\dot{\mathbf{H}}^{\text{da}} = \dot{\mu} \frac{\partial g^{\text{da}}}{\partial \tilde{\mathbf{T}}} = \dot{\mu} \alpha \mathbf{1} + \dot{\mu} \beta \frac{1}{2\sqrt{J_2}} \text{dev} \tilde{\mathbf{T}}. \tag{25}$$

The first term in Equation (25) represents inelastic volumetric deformations caused by the isotropic growth of microvoids, whereas the second term takes into account the significant dependence of the evolution of size, shape, and orientation of microdefects on the direction of stress simulating orthotropic damage behavior.

In addition, based on kinematic considerations (Brüning (2003a)) the identities

$$\dot{\mu} = \dot{f} \tag{26}$$

and

$$\alpha = \frac{1}{3} (1 - \check{f})^{-1} \tag{27}$$

hold, where  $\check{f}$  denotes the nonlocal generalization of the current void volume fraction (Tvergaard (1990)). Then, Equation (25) can be rewritten in the form

$$\dot{\mathbf{H}}^{\text{da}} = \dot{f} \frac{1}{3} (1 - \check{f})^{-1} + \dot{f} \beta \frac{1}{2\sqrt{J_2}} \text{dev} \tilde{\mathbf{T}}. \tag{28}$$

Based on experimental, theoretical, and numerical studies on iron-based metals Brüning (2003a) discussed realistic macroscopic damage propagation conditions. He proposed an isotropic damage model with  $\beta = \check{\beta} = 0$  in the early stage of material degradation until the void volume fraction reaches the critical value

$$f_c = 0.0344 + 1.25 \overset{o}{f} \tag{29}$$

which depends linearly on the initial porosity  $\overset{o}{f}$  of the material.

### COMPUTATIONAL ASPECTS

On the numerical side, a key factor in the numerical treatment of inelastic continuum models using the finite element method is the numerical

integration of the nonlinear constitutive equations governing the flow and damage behavior as well as the evolution of internal state variables.

For the numerical treatment of gradient-enhanced constitutive models in the context of the finite element method, Mühlhaus and Aifantis (1991), de Borst and Mühlhaus (1992), Sluys et al. (1993), and de Borst and Pamin (1996) presented finite element formulations and algorithms for a gradient plasticity model using mixed-type finite elements, thus satisfying the yield condition and the equilibrium conditions in a weak sense. In addition, Li and Cescotto (1996, 1997) and Brunet et al. (2004) presented a finite element model for a gradient plasticity approach in which the Laplacian of the effective plastic strain is evaluated at a quadrature point while the nonlocal yield condition is satisfied in a pointwise fashion. Strömberg and Ristinmaa (1996) also implemented a simplified nonlocal plasticity model into their finite element formulation but treated the consistency condition as an integral equation.

In the present study, however, estimates of the irreversible strain histories are obtained via an extended version of the inelastic predictor method (Nemat-Nasser, 1991; Brünig, 2003b). In the elastic corrector step the plastic and damage correctors,  $\Delta_{\text{er}}\hat{\gamma}$  and  $\Delta_{\text{er}}\hat{\mu}$ , are expanded in respective Taylor series, e.g.,

$$\Delta_{\text{er}}\hat{\gamma} = \Delta_{\text{er}}\gamma + d_{\text{pl}} \frac{\partial^2 \Delta_{\text{er}}\gamma}{\partial \mathbf{x} \cdot \partial \mathbf{x}} + \dots = \Delta_{\text{er}}\gamma + d_{\text{pl}} \nabla^2(\Delta_{\text{er}}\gamma) + \dots \quad (30)$$

for the plastic one where only terms up to second order are retained and  $d_{\text{pl}}$  takes into account a plastic internal length scale (Brünig et al., 2001). This leads to the system of coupled elliptic partial differential equations for the estimates of the correctors of the equivalent plastic and damage strains

$$m_{\text{pl}} d_{\text{pl}} \frac{\partial c}{\partial \gamma} \nabla^2(\Delta_{\text{er}}\gamma) + \left[ \sqrt{2} G_1 k_1 + \frac{\partial c}{\partial \gamma} \right] \Delta_{\text{er}}\gamma + \sqrt{2} G_1 k_2 \Delta_{\text{er}}\mu = c_{\text{pr}} - c(t) \quad (31)$$

and

$$m_{\text{da}} d_{\text{da}} \frac{\partial \sigma}{\partial \mu} \nabla^2(\Delta_{\text{er}}\mu) + \left[ \sqrt{2} G_2 k_4 + \frac{\partial \sigma}{\partial \mu} \right] \Delta_{\text{er}}\mu + \sqrt{2} G_2 k_3 \Delta_{\text{er}}\gamma = \sigma_{\text{pr}} - \sigma(t). \quad (32)$$

where  $G_1$  and  $G_2$  as well as  $k_1, \dots, k_4$  represent modified material parameters (Brünig and Ricci, 2005).  $c_{\text{pr}}$  and  $\sigma_{\text{pr}}$  are the equivalent stress measures computed at the end of the inelastic predictor step while  $c(t)$  and  $\sigma(t)$  denote the equivalent stress measures at the end of the former time

step, respectively. Equations (31) and (32) are solved via a standard finite difference method employing an overlay mesh defined by the Gaussian integration points of the underlying finite element mesh, whereas the global equilibrium equations are solved using standard displacement-based finite elements. At the end of each time step, equivalent plastic and damage strain increments are computed simultaneously which then lead to the corresponding tensorial quantities employing an integration scheme with an exponential shift.

Furthermore, the finite element procedure is based on the principle of virtual work and corresponding variational equations are obtained using a consistent linearization algorithm. The finite element formulation relies on quadrilaterals built up of four triangular elements with linear displacement fields.

### NUMERICAL SIMULATIONS

The numerical simulations deal with the finite deformation and localization behavior of uniaxially loaded rectangular aged maraging steel specimens. The material has been tested by Spitzig et al. (1976) and the elastic material behavior is described by the shear modulus  $G = 81,300$  MPa and the bulk modulus  $K = 166,300$  MPa whereas the rate-independent plastic material properties are adequately simulated by the saturation law

$$c = (c_s - c_0) \tanh\left(\frac{H_0 \tilde{\gamma}}{c_s - c_0}\right) + c_0. \quad (33)$$

Good agreement with test results is given with the initial yield stress  $c_0 = 870$  MPa, the initial hardening parameter  $H_0 = 96,000$  MPa and the saturation flow stress  $c_s = 1120$  MPa (see Brünig (1999) for further details) and the effect of superimposed hydrostatic stress on the flow characteristics of aged maraging steel in Equation (10) is chosen to be  $a/c = 20$  TPa<sup>-1</sup>. Due to numerical experiments the weighting parameters for nonlocality are chosen to be  $m_{pl} = m_{da} = 0.5$ . In addition, Spitzig et al. (1988) measured various elastic moduli of damaged and undamaged iron specimens. These experimental results are used to determine the material parameters  $\eta_1, \dots, \eta_4$  in Equation (22) and the respective values

$$\begin{aligned} \eta_1 &= -117500 \text{ MPa}, & \eta_2 &= -95000 \text{ MPa} \\ \eta_3 &= -190000 \text{ MPa}, & \eta_4 &= -255000 \text{ MPa} \end{aligned}$$

give the best fit to the experimental data (see Brünig (2003a)).

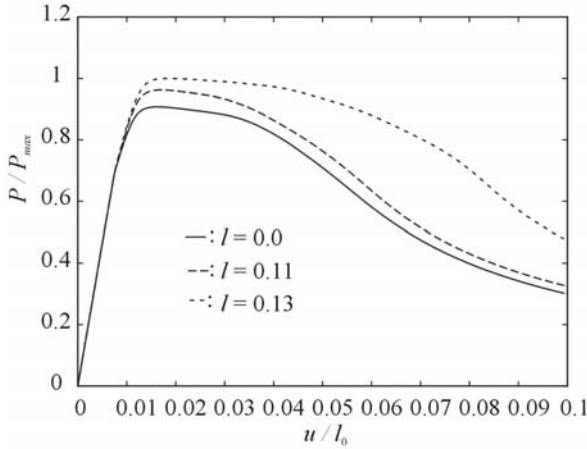


**Figure 1.** Load–deflection curves for different  $l = l_{pl} = l_{da}$ .

Furthermore, the equivalent aggregate stress–equivalent damage strain relationship is approximated by a piecewise linear curve with the respective slopes  $H^{da} = \partial\sigma/\partial f$ . These slopes are chosen to be  $H_1^{da} = -50$  MPa as long as  $f < f_c$  and  $H_2^{da} = -4000$  MPa for  $f \geq f_c$ .

Numerical calculations of uniaxially loaded rectangular specimens (initial length  $l_0$ /initial height  $h_0 = 4$ ) with clamped ends are carried out using displacement-based crossed-triangle elements. They take into account plane strain conditions and are based on the elastic–plastic–damage model with the constitutive parameters discussed earlier.

The corresponding load–deformation curves for different internal length parameters  $l = l_{pl} = l_{da}$  (see Equations (5) and (20)) are shown in Figure 1. In particular, the numerical calculation with  $l = 0$  (local model) shows a maximum load at  $u/l_0 = 0.015$ . The subsequent slight decrease in load corresponds to the formation of a neck whereas the later larger decrease is caused by the increase in damage. Similar load–deformation behavior is numerically predicted taking into account a nonlocal model with  $l = 0.11$  which only shows an increase in load of about 5%. Larger length parameters, however, lead to different load–deformation behavior. For example, the numerical calculation based on  $l = 0.13$  leads to larger loads for larger displacements which seems to be unrealistic. For the following numerical computations the characteristic length is chosen to be  $l = 0.056$  because for this value numerical experiments concerning the mesh dependence yield the best results. Here, the characteristic length is a weighted measure relative to the fineness of the mesh and is therefore dimensionless.

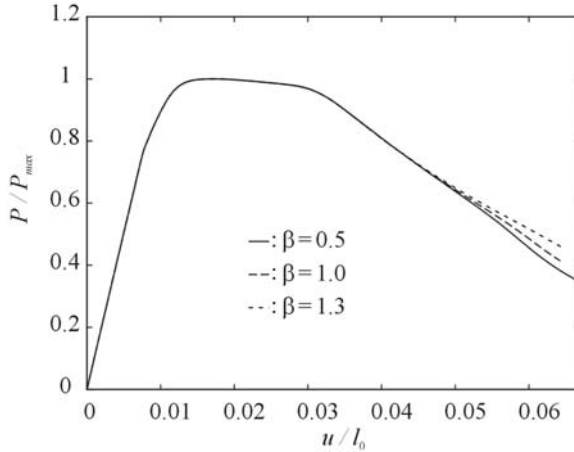


Figure 2. Load–deflection curves for different  $\beta$ .

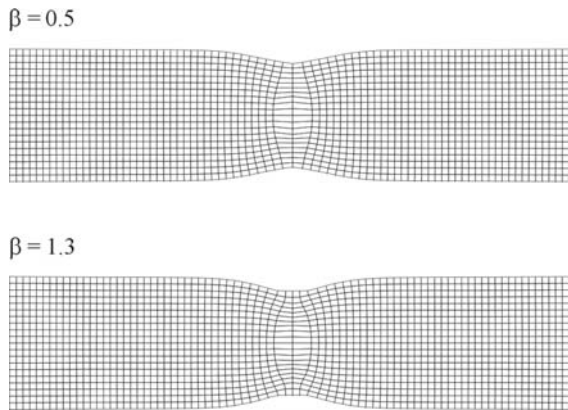


Figure 3. Deformed configurations.

Furthermore, the effect of the kinematic parameter  $\beta$  which appears in the damage rule (25) on the load–deformation behavior is shown in Figure 2. After the onset of anisotropic damage behavior ( $\bar{f} \geq f_c$ ) a larger decrease in load with further elongation is observed; but at the final elongation  $u/l_0 = 0.064$ , the difference in load is only of about 10%. In addition, Figure 3 shows the effect of increasing anisotropy on the deformation modes. Larger anisotropy ( $\beta = 1.3$ ) leads to more localized damage increase in the center region of the specimen which will lead to the initiation of a macrocrack in this region.

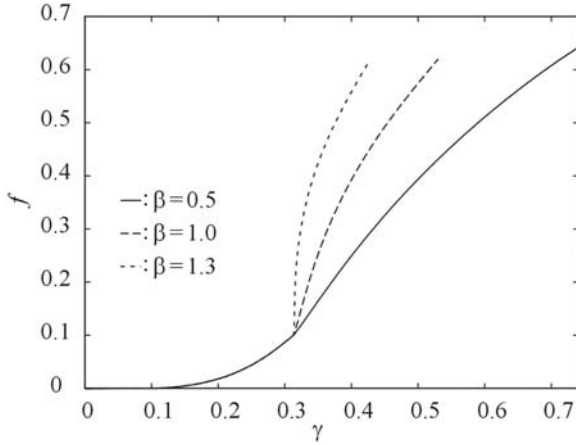


Figure 4. Void volume fraction vs equivalent plastic strains for different  $\beta$ .

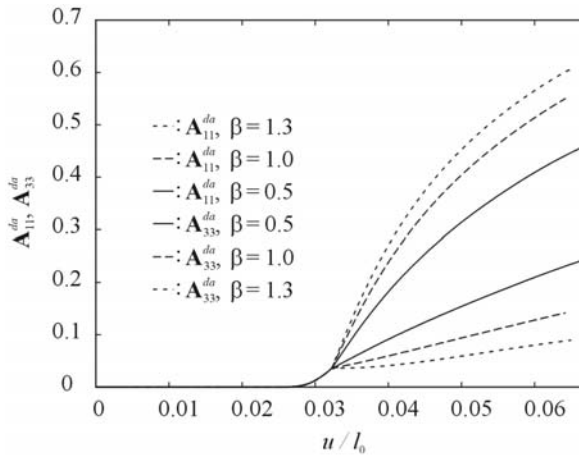


Figure 5. Influence of  $\beta$  on damage strains.

Moreover, the effect of anisotropy on damage variables in the center of the specimen is demonstrated in Figures 4 and 5. In particular, the increase in void volume fraction  $f$  (Figure 4) is remarkably larger with increasing anisotropy. This effect is also shown in Figure 5, where the difference between the evolution of damage strains in loading direction,  $A_{11}^{da}$  (upper curves), and normal to the loading direction,  $A_{33}^{da}$  (lower curves), becomes larger with increasing parameter  $\beta$ .

## CONCLUSIONS

A nonlocal anisotropic damage model for ductile metals and its numerical implementation, which is based on a nonlinear continuum damage mechanics approach, have been discussed, taking into account kinematic description of damage. The elastic constitutive equations are based on Helmholtz free energy functions of the fictitious undamaged configuration and of the current damaged configuration, respectively. The approach incorporates macroscopic interstate variables and their higher-order gradients which properly describe the change in the internal structure and investigate the size effect of statistical inhomogeneity of the heterogeneous material. The idea of bridging length-scales is made by introducing higher-order gradients in the evolution equations of the equivalent inelastic strain measures. A nonlocal macroscopic yield condition describes the plastic flow properties of ductile metals and a separate nonlocal damage criterion takes into account isotropic as well as anisotropic damage effects. Higher-order gradients in the evolution equations of the equivalent inelastic strain measures lead to a system of elliptic partial differential equations which are solved using the finite difference method. The applicability of the proposed continuum damage theory is demonstrated by the numerical simulation of the deformation behavior of ductile metals. The effect of anisotropic damage parameters on the numerically predicted deformation behavior of ductile metals has been discussed.

In conclusion, the present gradient-enhanced model offers a complementary alternative to conventional fracture mechanics and provides a comprehensive theory of anisotropic continuum damage mechanics capable of solving practical engineering problems including service life prediction of metal structures.

## REFERENCES

- Abu Al-Rub, R.K. and Voyiadjis, G.Z. (2003). On the Coupling of Anisotropic Damage and Plasticity Models for Ductile Materials, *Int. J. Solids Struct.*, **40**: 2611–2643.
- Abu Al-Rub, R.K. and Voyiadjis, G.Z. (2004). Analytical and Experimental Determination of the Material Intrinsic Length Scale of Strain Gradient Plasticity Theory from Micro- and Nano-indentation Experiments, *Int. J. Plasticity*, **20**: 1139–1182.
- Brünig, M. (1999). Numerical Simulation of the Large Elastic-plastic Deformation Behavior of Hydrostatic Stress-sensitive Solids, *Int. J. Plasticity*, **15**: 1237–1264.
- Brünig, M., Ricci, S. and Obrecht, H. (2001). Nonlocal Large Deformation and Localization Behavior of Metals, *Comput. Struct.*, **79**: 2063–2074.
- Brünig, M. (2003a). An Anisotropic Ductile Damage Model based on Irreversible Thermodynamics, *Int. J. Plasticity*, **19**: 1679–1713.
- Brünig, M. (2003b). Numerical Analysis of Anisotropic Ductile Continuum Damage, *Comput. Methods Appl. Mech. Engrg.*, **192**: 2949–2976.

- Brüning, M. and Ricci, S. (2005). Nonlocal Continuum Theory of Anisotropically Damaged Metals, *Int. J. Plasticity*, **21**: 1346–1382.
- Brunet, M., Morestin, F. and Walter, H. (2004). Damage Identification for Anisotropic Sheet-metals using a Non-local Damage Model, *Int. J. Damage Mech.*, **13**: 35–57.
- Chaboche, J.L. (1988a). Continuum Damage Mechanics: Part I – General Concepts, *J. Appl. Mech.*, **55**: 59–64.
- Chaboche, J.L. (1988b). Continuum Damage Mechanics: Part II – Damage Growth, Crack Initiation, and Crack Growth, *J. Appl. Mech.*, **55**: 65–72.
- de Borst, R. and Mühlhaus, H.B. (1992). Gradient-dependent Plasticity: Formulation and Algorithmic Aspects, *Int. J. Num. Meth. Eng.*, **35**: 521–539.
- de Borst, R. and Pamin, J. (1996). Some Novel Developments in Finite Element Procedures for Gradient-dependent Plasticity, *Int. J. Num. Meth. Eng.*, **39**: 2477–2505.
- Hammi, Y., Horstemeyer, M.F. and Bammann, D.J. (2003). An Anisotropic Damage Model for Ductile Metals, *Int. J. Damage Mech.*, **12**: 245–262.
- Hammi, Y., Bammann, D.J. and Horstemeyer, M.F. (2004). Modeling of Anisotropic Damage for Ductile Materials in Metal Forming Processes, *Int. J. Damage Mech.*, **13**: 123–146.
- Hayakawa, K., Murakami, S. and Liu, Y. (1998). An Irreversible Thermodynamics Theory for Elastic-plastic-damage Materials, *Eur. J. Mech., A/Solids*, **17**: 13–32.
- Ju, J.W. (1990). Isotropic and Anisotropic Damage Variables in Continuum Damage Mechanics, *J. Eng. Mech.*, **116**: 2764–2770.
- Kachanov, L.M. (1958). *On Rupture Time under Condition of Creep*, *Izvestia Akademi Nauk USSR, Otd. Techn. Nauk, Moskwa*, **8**: 26–31.
- Krajcinovic, D. (1983). Constitutive Equations for Damaging Materials, *J. Appl. Mech.*, **50**: 355–360.
- Lemaitre, J. (1985a). A Continuous Damage Mechanics Model for Ductile Fracture, *J. Eng. Mater. Tech.*, **107**: 83–89.
- Lemaitre, J. (1985b). Coupled Elasto-plasticity and Damage Constitutive Equations, *Comp. Meth. Appl. Mech. Eng.*, **51**: 31–49.
- Li, X. and Cescotto, S. (1996). Finite Element Method for Gradient Plasticity at Large Strains, *Int. J. Num. Meth. Eng.*, **39**: 619–633.
- Li, X. and Cescotto, S. (1997). A Mixed Element Method in Gradient Plasticity for Pressure Dependent Materials and Modelling of Strain Localization, *Comp. Meth. Appl. Mech. Eng.*, **144**: 287–305.
- Lubarda, V.A. and Krajcinovic, D. (1995). Some Fundamental Issues in Rate Theory of Damage-elastoplasticity, *Int. J. Plasticity*, **11**: 763–797.
- Mühlhaus, H.B. and Aifantis, E.C. (1991). A Variational Principle for Gradient Plasticity, *Int. J. Solids Struct.*, **28**: 845–857.
- Murakami, S. and Ohno, N. (1981). A Continuum Theory of Creep and Creep Damage, In: Ponter, A.R.S. and Hayhurst, D.R. (eds), *Creep in Structures*, Springer-Verlag, Berlin, pp. 422–443.
- Murakami, S. (1988). Mechanical Modeling of Material Damage, *J. Appl. Mech.*, **55**: 280–286.
- Nemat-Nasser, S. (1991). Rate-independent Finite-deformation Elastoplasticity: A New Explicit Constitutive Algorithm, *Mech. Mater.*, **11**: 235–249.
- Sluys, L.J., de Borst, R. and Mühlhaus, H.B. (1993). Wave Propagation, Localization and Dispersion in a Gradient Dependent Medium, *Int. J. Solids Struct.*, **30**: 1153–1171.
- Spitzig, W.A., Sober, R.J. and Richmond, O. (1976). The Effect of Hydrostatic Pressure on the Deformation Behavior of Maraging and HY-80 Steels and its Implications for Plasticity Theory, *Metall. Trans.*, **7A**: 1703–1710.
- Spitzig, W.A., Smelser, R.E. and Richmond, O. (1988). The Evolution of Damage and Fracture in Iron Compacts with Various Initial Porosities, *Acta Metall.*, **36**: 1201–1211.

- Strömberg, L. and Ristinmaa, M. (1996). FE-formulation of a Nonlocal Plasticity Theory, *Comp. Meth. Appl. Mech. Eng.*, **36**: 127–144.
- Tvergaard, V. (1990). Material Failure by Void Growth to Coalescence, *Adv. Appl. Mech.*, **27**: 83–151.
- Voyiadjis, G.Z. and Kattan, P.I. (1992). A Plasticity-damage Theory for Large Deformation of Solids - I. Theoretical Formulation, *Int. J. Eng. Science*, **30**: 1089–1108.